CLUSTERED WIRELESS SENSOR NETWORKS FOR ROBUST DISTRIBUTED FIELD RECONSTRUCTION BASED ON HYBRID SHIFT-INVARIANT SPACES

Günter Reise and Gerald Matz

Institute of Communications and Radio-Frequency Engineering, Vienna University of Technology
Gusshausstrasse 25/389, A-1040 Vienna, Austria; email: {greise,gmatz}@nt.tuwien.ac.at

ABSTRACT

We develop a clustered architecture for wireless sensor networks in order to perform distributed reconstruction of physical fields with low communication overhead. To this end, we introduce hybrid shift-invariant spaces which extend conventional shift-invariant spaces and allow for localized field reconstruction with a computational complexity that is linear in the number of sensors. In contrast to our previous work, this approach allows adaptation to portions of the field with different smoothness properties. In addition, we consider quantized measurements and imperfect knowledge of the sensor positions. Numerical simulations show that our method is robust against such non-idealities and offers significant performance advantages over global reconstruction.

1. INTRODUCTION

The interest in wireless sensor networks (WSN) has been steadily increasing in recent years due to their suitability for numerous monitoring tasks. WSN use remote sensors that are distributed over the region to be monitored in order to measure, process, and communicate information about the physical quantity of interest. In this paper, we deal with the reconstruction of physical fields from samples take by irregularly distributed sensors. This problem has been previously addressed in the literature mostly assuming that the field is (spatially) strictly bandlimited (BL). An efficient scheme for the reconstruction of BL fields using a trade-off between spatial oversampling and sensor quantizer resolution was developed in [1]. The accuracy of BL reconstruction in WSN using linear filters and non-uniform sampling was studied using random matrix theory in [2]. In conventional temporal sampling applications, sufficient band-limitation is ensured by preceding the sampling with an analog anti-aliasing filter. The main problem with the BL assumption in the context of WSN is the fact that i) many physical fields are non-BL by nature and ii) the spatial sampling cannot be preceded by analog anti-aliasing filters, as it is common with conventional temporal sampling schemes. In [3], it was found that significant oversampling is required to achieve small reconstruction errors when using BL reconstruction with non-BL fields.

In this paper, we pursue a new approach for the WSN problem of sampling and reconstructing non-BL fields introduced in [4]. This approach builds on the theory of *shift-invariant spaces* [5], which provide models for smooth fields without requiring strict band-limitation. In fact, non-wave fields (e.g. electrostatic fields, gravitation fields, diffusion fields) like those considered in [6] much resemble functions from non-BL shift-invariant spaces. In addition, with shift-invariant spaces there exist computationally efficient interpolation (reconstruction) algorithms for uniform and irregular sampling sets (sensor distributions). These algorithms are also highly local in that field reconstruction at a certain spatial position requires only samples from a small neighborhood. In [4] it was shown that shift-invariant spaces offer pronounced advantages over BL spaces. Specifically, their localized nature was exploited via a clustered WSN architecture to reduce the communication and computation requirements of field reconstruction. Here, we provide the following contributions that generalize and extend [4]:

- we introduce hybrid shift-invariant spaces that are based on using different generator functions in disjoint intervals (in the WSN context, the latter correspond to sensor clusters);
- we develop sampling and interpolation procedures in hybrid shift-invariant spaces, which are the basis for our field reconstruction techniques;
- we study how the quantization of measurements and imperfect knowledge of the sensor positions affect the stability and quality of field reconstruction.

The rest of the paper is organized as follows. In Section 2 we introduce our system architecture. In Section 3, we discuss shift-invariant spaces and their underlying generators. In Section 4, we outline the general approach for reconstruction in shift-invariant spaces and we then propose an efficient scheme implementing this reconstructions in a WSN assuming compactly supported generator functions. Section 5 illustrates the advantages of our approach via numerical simulations. Finally, Section 6 summarizes the main results.

2. WSN SYSTEM ARCHITECTURE

2.1. Sensor Clusters

Consider a WSN consisting of I sensors/nodes that are deployed over a certain region $\mathcal{A}$ to monitor a (scalar) physical field $h(x,y)$. We propose a clustered system architecture (see Fig. 1) where the region being monitored is divided into M subregions $\mathcal{A}_m$, $m = 1,\ldots,M$, such that $\bigcup_{m=1}^{M} \mathcal{A}_m = \mathcal{A}$. These subregions may overlap and may have different sizes. The I_m sensors within each subarea $\mathcal{A}_m$ form a cluster $\mathcal{C}_m$. Within each cluster, one node serves as cluster-head. The mth cluster-head collects the measurements from all nodes in the associated cluster $\mathcal{C}_m$ as well as their positions in order to reconstruct the field $h(x,y)$ within $\mathcal{A}_m$ (see Section 4). The case $M = 1$ corresponds to a centralized setup with a single fusion center.

We emphasize the distributed nature of our WSN architecture, i.e., only local communication and computation (within clusters) is required. The reconstruction within a cluster is performed independently of all other clusters. Thus, if the field reconstruction in a certain cluster is poor or fails, this has only a local effect and it is

Funded by FWF Grant N10606.

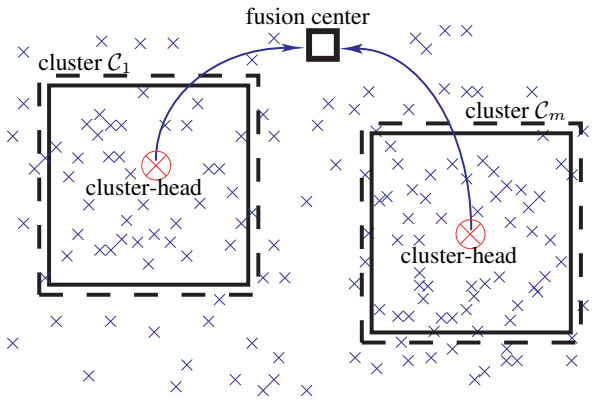

Fig. 1. *WSN architecture for field reconstruction. The field is reconstructed locally within each cluster. If desired, the result is forwarded to a fusion center.*

still possible to reconstruct $h(x,y)$ within $\mathcal{A}\backslash\mathcal{A}_m$. Moreover, it will be seen below that by exploiting the locality of our model, the complexity of field reconstruction is extremely low, i.e., only *linear* in the number of measurements (sensors).

The problem of how the clusters and cluster-heads are established (possible in a self-organized manner) is beyond the scope of this paper. The motivation for the clusters are reduced communication and computation efforts (see also Section 4.3) and a better adaptability to parts of the field $h(x,y)$ that feature different smoothness properties.

2.2. Sensor Placement

Of course, the field reconstruction quality depend strongly on the number of sensors and their placement. A uniform sensor placement on a sufficiently dense regular lattice is desirable but can hardly be achieved in practice. A more realistic deployment corresponds to jittered version of a regular spatial lattice, i.e., each sensor position corresponds to a slightly displaced lattice point. In [4] this was observed to require slightly larger sensor density. With even more sensors, the positioning requirements can be further relaxed and the sensor can be placed randomly.

In any case, the field reconstruction algorithm developed below requires that the positions of all sensors in a cluster are known to the respective cluster-head. This can be achieved using the localization techniques summarized e.g. in [7]. Hereby, each sensor determines an estimate of its position and communicates it to the associated cluster-head. Thus, the position information obtained by the cluster-head is affected by estimation and quantization errors. In the following, we assume that the position quantization error is negligible compared to the estimation error. This is motivated by the fact that our reconstruction algorithm (cf. Section 4) requires the sensor positions to be sent to the cluster head only once so that even with high quantizer resolution the associated communication overhead is negligible. The position estimate received[1] by the cluster-head is thus modeled as $(\hat{x}_i,\hat{y}_i) = (x_i+v_i, y_i+w_i)$, where (x_i,y_i) denotes the actual position of sensor i and $(v_i,w_i)\sim\mathcal{N}(\mathbf{0},\frac{\sigma^2}{2}\mathbf{I})$ is the corresponding estimation error, modeled as spatially i.i.d. Gaussian.

[1] We assume that the transmission of the position estimate is error-free.

2.3. Sensor Measurements

The measurements taken by the individual sensors correspond to samples $h(x_i,y_i)$, $i=1,\ldots,I$, of the physical field to be monitored. We assume that each sensor uses a uniform quantizer with a resolution of B bits and dynamic range $\pm h_{\max}$ in order to store and transmit its measurements. The quantized measurements are given by $h_i = Q\{h(x_i,y_i)+z_i\}$, where $Q\{\cdot\}$ represents the action of the quantizer and z_i denotes measurement noise. If the quantizer dynamic range is large enough to avoid clipping, the maximum quantization error is thus given by $2^{-B+1}h_{\max}$. The quantizer resolution B thus will impact the field reconstruction quality but also the communication requirements for transmitting the measurements to the cluster head. Since typically many measurements will be taken over time, the choice of B can have a significant impact on network lifetime, since repeated transmission of a large number of bits may eat up a significant fraction of sensor battery power.

3. HYBRID SHIFT-INVARIANT SPACES AND NON-WAVE FIELDS

In order to formulate our field reconstruction algorithm, we next introduce the novel notion of *hybrid shift-invariant spaces* that extend ordinary shift-invariant spaces as discussed e.g. in [5]. Throughout the paper, we will restrict our discussion to the two-dimensional (2-D) case.

Consider a partition of $\mathbb{Z}^2$ into disjoint sets $\mathbb{A}_m$, $m=1,\ldots,M$, i.e., $\mathbb{Z}^2=\bigcup_{m=1}^M\mathbb{A}_m$, $\mathbb{A}_m\cap\mathbb{A}_l=\emptyset$, $m\neq l$, and associate a square-integrable[2] generator function $g_m(x,y)\in L^2(\mathbb{R}^2)$ to each subset. In the context of our WSN we will choose $\mathbb{A}_m=\mathcal{A}_m\cap\mathbb{Z}^2$. The corresponding hybrid shift-invariant space is then defined as

$$V(\mathcal{G})=\left\{f(x,y)\colon\ f(x,y)=\sum_{m=1}^{M}\sum_{(k,l)\in\mathbb{A}_m}c_{k,l}\,g_m(x-k,y-l)\right\}, \tag{1}$$

where $\mathcal{G}=\{g_m(x,y)\}_{m=1,\ldots,M}$ and $c_{k,l}\in l_2(\mathbb{Z}^2)$. This defines a linear subspace of $L^2(\mathbb{R}^2)$ that comprises all fields that can be represented as weighted superposition of spatial translates of the generator functions $g_m(x,y)$. To guarantee the stability of (1), we assume that the set $\bigcup_{m=1}^M\big\{g_m(x-k,y-l)\big)\big\}_{(k,l)\in\mathbb{A}_m}$ forms a Riesz basis for $V(\mathcal{G})$ (cf. [5]). Using different generator functions $g_m(x,y)$ for the sets $\mathbb{A}_m$ allows to locally adapt the smoothness properties of the functions in $V(\mathcal{G})$. Conventional shift invariant spaces are re-obtained as special case with identical generators, i.e., $g_1(x,y)=g_2(x,y)=\cdots=g_M(x,y)$.

For reasons of computation complexity (see Section 4), it is highly desirable to use generator functions with compact support, i.e. $\operatorname{supp} g_m\subseteq[-S_m/2,S_m/2]\times[-S_m/2,S_m/2]$. Here, the support of $g_m(x,y)$ is defined as

$$\operatorname{supp} g_m\triangleq\operatorname{cl}\big\{(x,y)\in\mathbb{R}^2\colon\ |g_m(x,y)|>0\big\},$$

where $\operatorname{cl}\{\cdot\}$ denotes topological closure. A particularly useful class of compactly supported generator functions is given by basis-splines (B-splines). Specifically, we will use 2-D spline functions in the following, constructed as $b_n(x,y)=\tilde{b}_n(x)\tilde{b}_n(y)$, with the one-

[2] We denote the space of square-integrable 2-D functions by $L^2(\mathbb{R}^2)=\{f(x,y)\colon\int_{\mathbb{R}^2}|f(x,y)|^2dx\,dy<\infty\}$, and the space of square-summable 2-D sequences by $l_2(\mathbb{Z}^2)=\{c_{k,l}\colon\sum_{(k,l)\in\mathbb{Z}^2}|c_{k,l}|^2<\infty\}$.

dimensional splines of order n defined via the n-fold convolution

$$\tilde{b}_n(x) \triangleq \Pi(x) \underbrace{* \Pi(x) \ldots * \Pi(x)}_{n \text{ times}}, \tag{2}$$

with the rectangular function $\Pi(x) = \tilde{b}_0(x)$ defined as

$$\Pi(x) \triangleq \begin{cases} 1, & |x| \leq \frac{1}{2}, \\ 0, & \text{else.} \end{cases}$$

The support of the 2-D splines equals $\operatorname{supp} b_n = [-(n+1)/2, (n+1)/2] \times [-(n+1)/2, (n+1)/2]$. It is important in our application context to note that due to the compact support of splines the hybrid shift-invariant spaces $V(\mathcal{G})$ they induce are *not* BL and highly *local*. Locality here means that according to the representation $f(x,y) = \sum_{m=1}^{M} \sum_{(k,l)\in\mathbb{A}_m} c_{k,l}\, g_m(x-k, y-l)$ with $g_m(x,y) = b_{n(m)}(x,y)$, the field value $f(x_0, y_0)$ at any position $(x_0, y_0) \in \mathcal{A}$ depends on at most $(N+1)^2$ coefficients (here, $N = \max\{n(m)\}_{m=1,\ldots,M}$ denotes the largest spline order occurring in $V(\mathcal{G})$). In the rest of this paper, we will restrict to splines as generator functions for our hybrid shift-invariant spaces.

3.1. Non-Wave Fields

The physical field to be monitored with our WSN are usually governed by differential equations and in most cases are not BL. To check the suitability of hybrid shift-invariant spaces as field models, we study the simple fields that were considered in [6] in a sensor array context. Here, P sources induce a non-wave field given by

$$h(x,y) = \sum_{p=1}^{P} A_p\, q\Big(\frac{x-x_p}{D_p}, \frac{y-y_p}{D_p}\Big), \tag{3}$$

where A_p and (x_p, y_p) denote the amplitude and position of the pth source, respectively, $q(x,y)$ characterizes the initial field induced by a normalized source located at the origin, and the D_p are scale parameters that account for the different activation times of the sources. The model (3) can be used e.g. for electrostatic and gravitation fields by setting $q(x,y) = \frac{1}{\sqrt{1+x^2+y^2}}$ and for diffusion fields in liquids and gases with the choice

$$q(x,y) = \mathrm{e}^{-(x^2+y^2)}\ . \tag{4}$$

In the simulations section, we will focus on diffusion fields, an example of which is shown in Fig. 2. Note that in the case $(x_p, y_p) \in \mathbb{Z}^2$, the field $h(x,y)$ in (3) is an element of a hybrid shift-invariant space with $M = P$ generators $g_m(x,y) = q\big(\frac{x}{D_m}, \frac{y}{D_m}\big)$. Indeed, the field coefficients in this case are given by $c_{x_p,y_p} = A_p$, $p = 1, \ldots, P$, and $c_{k,l} = 0$ otherwise. These observations suggest that the hybrid shift-invariant spaces we introduced above are well-suited to model non-wave fields in more general cases than captured by (3) (e.g. inhomogeneous and possibly non-linear media).

4. FIELD RECONSTRUCTION

4.1. Reconstruction Scheme

Our field reconstruction method is an extension of [8] to hybrid shift-invariant spaces in two dimensions. Assuming that the field $h(x,y)$ belongs to a hybrid shift invariant space $V(\mathcal{G})$, the reconstruction of $h(x,y)$ from the sensor measurements h_i (cf. Section 2.3) amounts

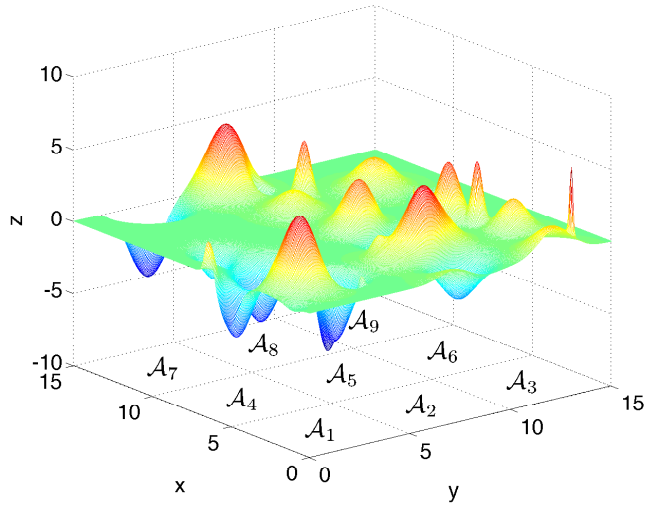

Fig. 2. *Example for a diffusion field monitored by a sensor network with 9 clusters (corresponding to sub-regions $\mathcal{A}_1, \ldots, \mathcal{A}_9$).*

to determining the coefficients $c_{k,l}$. In the case of spline generators with compact support, the localized nature of $V(\mathcal{G})$ entails that the coefficients $c_{k,l}$ can be computed separately for any subset $\mathbb{A}_m$. This means that all cluster-heads can independently perform local field reconstruction with their associated regions $\mathcal{A}_m$, $m = 1, \ldots, M$. Hence, in the following we will only consider reconstruction within one sub-region $\mathcal{A}_m$ and associated cluster $\mathcal{C}_m$. We denote by $I_m = |\mathcal{C}_m|$ the number of sensors in the cluster and, for simplicity of exposition, assume error-free measurements and perfectly known sensor positions, i.e., $h_i = h(x_i, y_i)$ and $(\hat{x}_i, \hat{y}_i) = (x_i, y_i)$, as well as rectangular sub-regions $\mathcal{A}_m$.

Denoting the maximum spline order in $V(\mathcal{G})$ by N, any field value $h(x', y')$ is completely determined by the coefficients $c_{k,l}$ in the neighborhood $(x', y') + \mathcal{S}$ with $\mathcal{S} \triangleq [-(N+1)/2, (N+1)/2] \times [-(N+1)/2, (N+1)/2]$. Thus, reconstruction within $\mathcal{A}_m$ requires only the coefficients $c_{k,l}$ lying within $\mathcal{A}_m + \mathcal{S}$, i.e., for $(k,l) \in \mathbb{Z}^2_m \triangleq \mathbb{Z}^2 \cap (\mathcal{A}_m + \mathcal{S})$. Correspondingly, least-squares field reconstruction amounts to minimizing

$$\sum_{i\in\mathcal{C}_m} \Big| \sum_{(k,l)\in\mathbb{Z}^2_m} c_{k,l}\, g_{m(k,l)}(x_i - k, y_i - l) \;-\; h_i \Big|^2 \tag{5}$$

with respect to $c_{k,l}$, $(k,l) \in \mathbb{Z}^2_m$. Here, $m(k,l)$ is the index of the generator function associated to (k,l). The problem (5) leads to a system of linear equations (see below) which can be solved provided that $I_m \geq J_m \triangleq |\mathbb{Z}^2_m|$, i.e., at least J_M sensors are required within $\mathcal{A}_m$. Once the optimum coefficients $\hat{c}_{k,l}$ have been computed, the field within $\mathcal{A}_m$ can be reconstructed as

$$\hat{h}(x,y) = \sum_{k,l\in\mathbb{Z}^2_m} \hat{c}_{k,l}\, g_{m(k,l)}(x-k, y-l), \quad (x,y) \in \mathcal{A}_m. \tag{6}$$

Alternatively, each cluster-head may forward its estimated coefficients to a fusion center which performs global reconstruction for all clusters.

4.2. Matrix Formulation

We next provide a reformulation of field reconstruction in terms of matrices and vectors. Let (k_0, l_0) and (k_1, l_1) denote the smallest

and largest indices, respectively, in $\mathbb{Z}_m^2$ such that $J_m = K(l_1 - l_0 + 1)$ with $K \triangleq k_1 - k_0 + 1$. We define the $I_m \times J_m$ matrix

$$[\mathbf{G}]_{j,r+1} = g_{m(k_r,l_r)}\big(x_{i_j} - k_r,\, y_{i_j} - l_r\big), \tag{7}$$

where i_j, $j = 1, \ldots, I_m$, denotes the indices of the sensors located in $\mathcal{A}_m$ (i.e., $\mathcal{C}_m = \{i_1, \ldots, i_{I_m}\}$), $k_r = k_0 + ((r-1) \bmod K)$, and $l_r = l_0 + \lfloor \frac{r}{K} \rfloor$ (here, $r = 0, \ldots, J_m - 1$ and $\lfloor t \rfloor$ denotes the largest integer not larger than t). We emphasize that $\mathbf{G}$ will be a sparse matrix whenever $\mathcal{A}_m$ is larger than $\mathcal{S}$. Indeed, $g_{m(k_r,l_r)}\big(x_{i_j} - k_r,\, y_{i_j} - l_r\big) \neq 0$ only if $|x_{i_j} - k_r| \leq (N+1)/2$ or $|y_{i_j} - l_r| \leq (N+1)/2$, which can happen for at most $|\mathcal{S}| = (N+1)^2$ of the J_m elements in each row.

Corresponding to (7), the measurements and unknown coefficients are arranged into respective vectors $\mathbf{h}$ and $\mathbf{c}$ according to

$$[\mathbf{h}]_j = h_{i_j}\,, \qquad [\mathbf{c}]_{r+1} = c_{k_r,l_r}\,. \tag{8}$$

These definitions allow to rewrite the minimization problem (5) as

$$\hat{\mathbf{c}} = \arg\min_{\mathbf{c}} \|\mathbf{G}\mathbf{c} - \mathbf{h}\|.$$

The optimum coefficient vector $\hat{\mathbf{c}}$ is thus obtained as solution to the associated normal equations [9],

$$\mathbf{G}^H\mathbf{G}\,\hat{\mathbf{c}} = \mathbf{G}^H\mathbf{h}\,,$$

i.e., $\hat{\mathbf{c}} = (\mathbf{G}^H\mathbf{G})^{-1}\mathbf{G}^H\mathbf{h}$. We note that this presupposes $\mathbf{G}^H\mathbf{G}$ to be invertible, which is equivalent to the requirement that there have to be enough appropriately spaced sensors sampling the field. Technically, the sensor positions (x_i, y_i), $i \in \mathcal{C}_m$, have to form a stable sampling set (cf. [8]). For the one-dimensional case, stable sampling sets for B-spline spaces are well understood. This is not true for the 2-D case, where only probabilistic statements have been obtained recently [10].

4.3. Algorithm and Complexity

In the following, we summarize all algorithmic steps necessary to perform field reconstruction and we provide estimates for their computational complexity.

Preprocessing. Solving the normal equations requires computation of the positive semi-definite $J_m \times J_m$ matrix $\mathbf{T} = \mathbf{G}^H\mathbf{G}$:

$$[\mathbf{T}]_{s,r} = \sum_{j=1}^{I_m} g^*_{m(k_s,l_s)}(x_{i_j} - k_s, y_{i_j} - l_s)\, g_{m(k_r,l_r)}(x_{i_j} - k_r, y_{i_j} - l_r).$$

Here, superscript * denotes complex conjugation. Due to the compact support of $g_m(x,y)$ and the corresponding sparsity of $\mathbf{G}$, it follows that $\mathbf{T}$ is also sparse. Since $\mathbf{T}$ is sparse and positive definite, the normal equations can efficiently be solved using a sparse LDL factorization [9], i.e., $\mathbf{T} = \mathbf{L}\mathbf{D}\mathbf{L}^T$. Both, the calculation and the factorization of $\mathbf{T}$ need $\mathcal{O}(I_m(N+1)^4)$ operations. Note that the computation of $\mathbf{T}$ requires only the sensor positions and the generator functions and can hence be performed by the cluster-head in the initialization phase of the WSN, i.e., before any actual measurements h_i are obtained.

Field reconstruction. First, $\bar{\mathbf{h}} = \mathbf{G}^H\mathbf{h}$ is computed according to

$$[\bar{\mathbf{h}}]_r = \sum_{j=1}^{I_m} g^*_{m(k_r,l_r)}(x_{i_j} - k_r, y_{i_j} - l_r)\, h_{i_j}.$$

The sparsity of $\mathbf{G}$ resulting from the compact support of $g_m(x,y)$ allows to perform this step with $\mathcal{O}(I_m(N+1)^2)$ operations. Finally, we solve the normal equations $\mathbf{T}\hat{\mathbf{c}} = \bar{\mathbf{h}}$ using the pre-computed sparse LDL factorization of $\mathbf{T}$. This amounts to solving $\mathbf{L}\mathbf{D}\mathbf{L}^T\mathbf{c} = \bar{\mathbf{h}}$ via forward elimination and back substitution [9]. The coefficients $\mathbf{c}$ are therefore obtained with complexity $\mathcal{O}(I_m(N+1)^4)$. Finally, the field can be reconstructed at any point $(x,y) \in \mathcal{A}_m$ according to (6). This requires $\mathcal{O}((N+1)^2)$ operations per spatial point.

We conclude that the overall complexity of our scheme scales linearly with the number of sensor, independently of the specific clustering. In order to distribute computations as much as possible, many small clusters appear desirable, which also reduces the communication requirements. However, with small clusters the condition $I_m \geq J_m$ tends to be violated (and thus reconstruction fails locally) more and more often.

5. NUMERICAL SIMULATIONS

We next present numerical results to illustrate the performance of our distributed field reconstruction scheme. The simulated WSN was deployed over the square region $\mathcal{A} = [0,15] \times [0,15]$. We consider three different types of sensor placements:

i) regular: exact placement on a rectangular lattice $(d_x\, k, d_y\, l) \cap \mathcal{A}$ with $k, l \in \mathbb{Z}$;

ii) jittered: similar to i) but with jitter (the jitters were i.i.d. uniform within $[-d_x/4, d_x/4] \times [-d_y/4, d_y/4]$);

iii) random: random sensor placement, uniformly distributed in $\mathcal{A}$.

Our WSN architecture used $M = 9$ clusters corresponding to the square sub-regions $\mathcal{A}_1 = [0,5] \times [0,5]$, $\mathcal{A}_2 = [0,5] \times [5,10]$, $\mathcal{A}_3 = [0,5] \times [10,15]$, $\mathcal{A}_4 = [5,10] \times [0,5]$ $\mathcal{A}_5 = [5,10] \times [5,10]$, $\mathcal{A}_6 = [5,10] \times [10,15]$, $\mathcal{A}_7 = [10,15] \times [0,5]$, $\mathcal{A}_8 = [10,15] \times [5,10]$, and $\mathcal{A}_9 = [10,15] \times [10,15]$ (see Figure 2). Within each cluster, we used spline generators with order ranging from 1 to $N = 8$.

We created random diffusion fields according to (3) and (4), with uniformly distributed $P \sim \text{Unif}[0,50]$, uniformly distributed $A_p \sim \text{Unif}[-10,10]$, uniformly distributed $D_p \sim \text{Unif}[0,\sqrt{1.5}]$, and source positions (x_p, y_p) uniformly distributed in $\mathcal{A}$. Observation noise was neglected against quantization errors. Field reconstruction was then performed for every sub-region $\mathcal{A}_m$ with the algorithm described in Section 4.3 based on hybrid shift-invariant spaces induced by splines of optimum order (determined empirically) for each cluster. For comparison, we show results obtained using the same (globally optimum) generator in all clusters, which corresponds to a conventional shift-invariant space. The performance measure employed is the normalized mean square error[3] (MSE) defined as $\text{MSE} = \text{E}\{\|\hat{h} - h\|^2\}/\text{E}\{\|h\|^2\}$.

Spline order and quantization. We first present results obtained with a WSN consisting of $I = 70^2 = 4900$ regularly placed sensors, whose positions are exactly known to the cluster-heads. Furthermore, the same spline order was used in each cluster (amounting to a conventional shift-invariant space). Fig. 3(a) shows the MSE versus the spline order for different quantizer resolutions $B \in \{4, 6, 8\}$. It is seen that there is a significant MSE improvement when going from $B = 4$ to $B = 6$; however, there is little to be gained from using $B = 8$ bits per measurement. This suggest that 6-bit quantization is sufficient in this setup. Furthermore, there is no distinct MSE minimum regarding the spline order, i.e., choosing n between 5 and 8 leads to effectively identical performance. This can be attributed to the fact that the field consists of wide as well as narrow pulses, for which different spline orders would be advantageous.

[3] Here, $\text{E}\{\cdot\}$ denotes mathematical expectation.

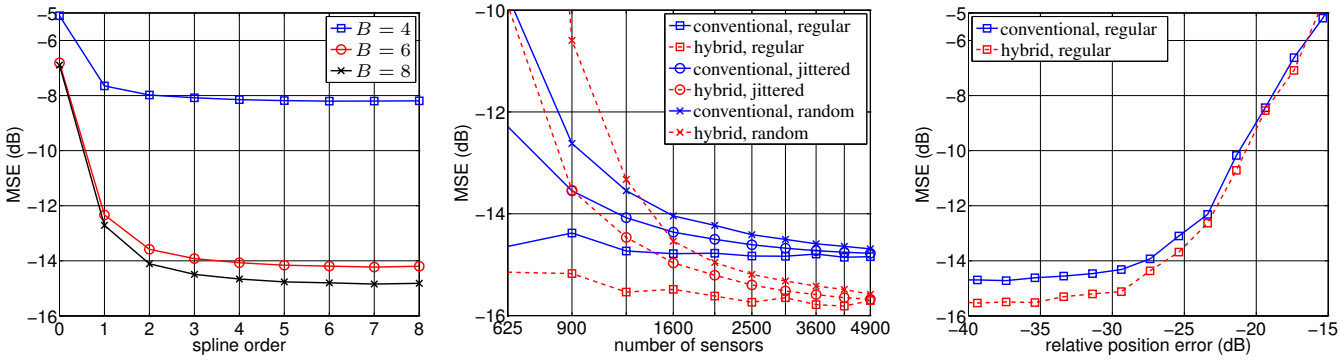

Fig. 3. *(a) MSE versus spline order for $B \in \{4, 6, 8\}$, regular placement of 4900 sensors, and identical generator in all clusters; (b) MSE versus number of sensors for conventional and hybrid reconstruction and various sensor placements ($B = 8$); (c) MSE versus relative position error for conventional and hybrid reconstruction and regular placement of 4900 sensors.*

Hybrid versus conventional shift-invariant spaces. We next study the gains achievable by using different generators (i.e., different spline orders) in the individual clusters. To this end, Fig. 3(b) shows the field reconstruction MSE versus the number of sensors achieved for different sensor placements (regular, jittered, random) based on i) conventional shift-invariant spaces using the the same (optimal) spline order in all clusters (labeled 'conventional') and ii) on hybrid shift-invariant spaces using different (locally optimal) spline orders (labeled 'hybrid'). In all cases, $B = 8$ bits were used for the quantization of the sensor measurements and the sensor positions were exactly known to the cluster-heads. All MSE curves saturate with increasing number of sensors due to the (small) mismatch between (hybrid) shift-invariant spaces and the actual field. However, for all three types of sensor placements "hybrid" reconstruction has a lower MSE saturation level than "conventional" reconstruction with a gain of roughly 1 dB for sufficiently many sensors. This rather small gain can be attributed to the fact that there are only $M = 9$ clusters but up to $P = 50$ diffusion sources. If M is chosen roughly equal to P, the gain achievable with "hybrid" reconstruction can be significantly larger. Furthermore, it is seen that for small number of sensors jittered and random sensor placement lead to higher MSE than regular placement; this can be attributed to the fact that jittered/random placement more often leads to sampling sets that are not stable (cf. [8]).

Position estimation error. Fig. 3(c) shows the MSE versus the relative error of the sensor position estimates, defined as $\varepsilon^2 = \frac{\sigma^2}{2d_x^2} + \frac{\sigma^2}{2d_y^2}$, for a WSN with 4900 regularly placed sensors (similar results were obtained with jittered and random placement). It is seen that for small ε^2, there is virtually no effect on the field reconstruction quality. For $\varepsilon^2 \geq -26$ dB, however, the reconstruction error increases rapidly, indicating that a relative positioning accuracy of about 5% is required to avoid performance loss.

6. CONCLUSION

We proposed a clustered sensor network architecture for sampling and reconstruction of non-wave fields. Our approach is based on the novel concept of hybrid shift-invariant spaces, extending the theory and algorithms developed recently for shift-invariant spaces. The major advantages of our scheme are excellent reconstruction quality, a computational complexity that is only linear in the number of sensors and can be nicely distributed over the clusters, low communication overhead (due to the clustered architecture), and robustness against measurement quantization errors and sensor position uncertainty. In our future research, we plan to work on automated cluster and generator adaptation to trade performance versus network lifetime and on the inclusion of temporal field dynamics.

REFERENCES

[1] P. Ishwar, A. Kumar, and K. Ramchandran, "Distributed sampling in dense sensor networks: a 'bit-conservation principle'," in *Proc. IEEE Int. Symp. Information Processing in Sensor Networks*, Palo Alto, CA, April 2003, pp. 17–31.

[2] A. Nordio, C. F. Chiasserini, and E. Viterbo, "Performance of linear field reconstruction techniques with noise and uncertain sensor locations," *IEEE Trans. Signal Processing*, vol. 56, pp. 3535–3547, Aug. 2008.

[3] A. Kumar, P. Ishwar, and K. Ramchandran, "On distributed sampling of smooth non-bandlimited fields," in *Proc. IEEE Int. Symp. Information Processing in Sensor Networks*, Berkeley, CA, April 26–27, 2004, pp. 89–98.

[4] G. Reise and G. Matz, "Distributed sampling and reconstruction of non-bandlimited fields in sensor networks based on shift-invariant spaces," accepted for ICASSP, 2009.

[5] A. Aldroubi and K. Gröchenig, "Nonuniform sampling and reconstruction in shift-invariant spaces," *SIAM Rev.*, , no. 4, pp. 585–620, 2001.

[6] Alex B. Gershman and Victor I. Turchin, "Nonwave field processing using sensor array approach," *Signal Processing*, vol. 44, pp. 197–210, 1994.

[7] G. Mao, B. Fidan, and B.D.O. Anderson, "Wireless sensor network localization techniques," *Computer Networks: The International Journal of Computer and Telecommunications Networking*, vol. 51, no. 10, pp. 2529–2553, 2007.

[8] K. Gröchenig and H. Schwab, "Fast local reconstruction methods for nonuniform sampling in shift-invariant spaces," *SIAM J. Matrix Anal. Appl.*, vol. 24, no. 4, pp. 899–913, April 2003.

[9] G. H. Golub and C. F. Van Loan, *Matrix Computations*, Johns Hopkins University Press, Baltimore, 3rd edition, 1996.

[10] K. Gröchenig and R. F. Bass, "Random sampling of entire functions of exponential type in several variables," arXiv:0706.3818v2, 2008.